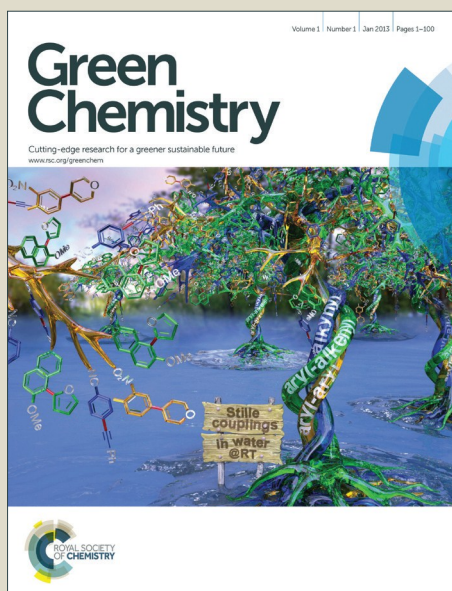


# Green Chemistry

Accepted Manuscript



This article can be cited before page numbers have been issued, to do this please use: J. Zhang, Y. Cai, G. Lu and C. Cai, *Green Chem.*, 2016, DOI: 10.1039/C6GC02265K.



This is an *Accepted Manuscript*, which has been through the Royal Society of Chemistry peer review process and has been accepted for publication.

*Accepted Manuscripts* are published online shortly after acceptance, before technical editing, formatting and proof reading. Using this free service, authors can make their results available to the community, in citable form, before we publish the edited article. We will replace this *Accepted Manuscript* with the edited and formatted *Advance Article* as soon as it is available.

You can find more information about *Accepted Manuscripts* in the [Information for Authors](#).

Please note that technical editing may introduce minor changes to the text and/or graphics, which may alter content. The journal's standard [Terms & Conditions](#) and the [Ethical guidelines](#) still apply. In no event shall the Royal Society of Chemistry be held responsible for any errors or omissions in this *Accepted Manuscript* or any consequences arising from the use of any information it contains.



## Green Chemistry

## COMMUNICATION

# Facile and selective hydrogenolysis of $\beta$ -O-4 linkages in lignin catalyzed by Pd-Ni bimetallic nanoparticles supported on $ZrO_2$

Received 00th January 20xx,  
Accepted 00th January 20xx

DOI: 10.1039/x0xx00000x

www.rsc.org/

Jia-wei Zhang, Yao Cai, Guo-ping Lu,\* and Chun Cai\*

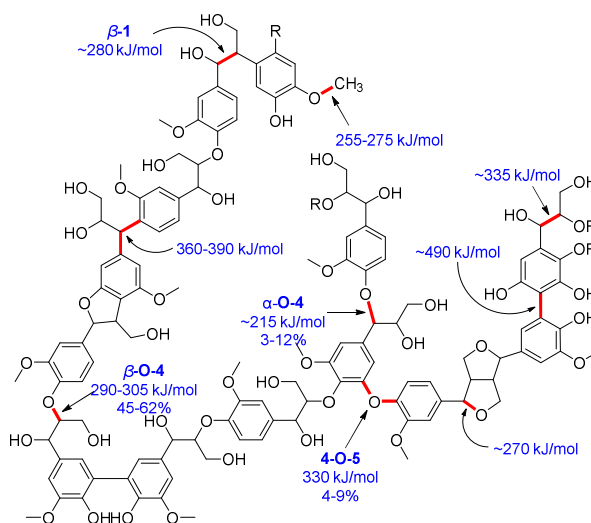
The  $\beta$ -O-4 linkage in lignin can be selectively cleaved by Pd-Ni bimetallic nanoparticles supported on  $ZrO_2$  using hydrogen gas as the hydrogen donor under ambient pressure and neutral conditions. Conspicuous enhancement in activity is observed compared with single nickel and palladium catalysts based on the results of experiments and characterization. Moreover, hydrogenation of the produced phenols is tuned by adjusting the amount of  $NaBH_4$ . The catalyst can be reused over ten times in the model reaction and over five times in the hydrogenolysis of lignin without an obvious change in activity and selectivity.

## Introduction

Lignocellulosic biomass has attracted plenty of attention as a substantial feedstock for production of fuels and chemicals in place of fossil fuels (petroleum, coal and natural gas) due to its abundant reserves and high-energy outputs.<sup>1</sup> Until now, commercial biochemical conversions mainly concentrate on utilization of cellulosic components,<sup>2</sup> leaving valorization processes of lignin limited, which means that 40% energy of lignocellulosic biomass is still waiting for exploitation.<sup>3</sup> Furthermore, lignin is the only large-volume renewable feedstock that is composed of aromatics and typically viewed as a waste stream in current biorefinery processes,<sup>4</sup> so utilization of lignin with high efficiency not only makes contributions to the petroleum crisis and to being economically viable, but also relieves the solid waste disposal problem.<sup>5</sup>

Lignin is an amorphous polymer of methoxylated phenylpropane units mainly bonded through several types of  $C_{aryl}$ -O linkages with the most abundant being the  $\beta$ -O-4 ether linkages (Scheme 1).<sup>6</sup> Typically,  $C_{aryl}$ -O bonds are relatively weaker and more labile than C-C bonds, so the cleavage of

$C_{aryl}$ -O bonds in lignin is a facile alternative approach for lignin depolymerization.<sup>7</sup> Among reported methods for the dissociation of  $C_{aryl}$ -O linkages, the hydrogenolysis process is one of the most promising options.<sup>8</sup> On one hand, catalysts based on noble metal elements are often characterized by high activity for transformation of hydrogen, which is beneficial to the hydrogenolysis of  $C_{aryl}$ -O linkages while the hydrogenation of the aromatic rings is also enhanced resulting in poor selectivity.<sup>3d,9</sup>



**Scheme 1** Representative structure of a fragment of lignin, showing the most frequent ether linkages and their abundance in percent.

On the other hand, a series of reports have mentioned that nickel catalysts show excellent selectivity in the cleavage of  $C_{aryl}$ -O ether linkage.<sup>10</sup> Nevertheless, poor activity and stability limit their applications in lignin depolymerization.<sup>11</sup> Therefore, quest for an ideal catalyst is still ongoing. Bimetallic nanoparticles (BMNPs), usually show a combination of the properties associated with two different metals<sup>12</sup> and performance superior to their monometallic counterparts due

Chemical Engineering College, Nanjing University of Science & Technology  
Xiaolingwei 200, Nanjing 210094, P. R. China  
E-mail: glu@njust.edu.cn, c.cai@njust.edu.cn

Electronic Supplementary Information (ESI) available: [details of any supplementary information available should be included here]. See DOI: 10.1039/x0xx00000x

## COMMUNICATION

Journal Name

to a phenomenon collectively referred as “synergistic effects”<sup>13</sup>, seem to be the foremost candidates. On the basis of those reports, we reason that Ni-based BMNPs, which may inherit the advantages of both metals as well as showing some superior properties, can be an ideal catalyst to achieve this goal.

Yan’s group has made initial attempts on this area,<sup>10c,14</sup> in which series of Ni-based BMNPs were prepared and applied in the hydrogenolysis of the  $\beta$ -O-4 ether linkages in lignin, and those BMNPs were proved to be more active and selective than their single component counterparts in the hydrogenolysis of lignin model compounds and real lignin. Inspired by their outstanding works, herein, we prepared a recyclable Pd-Ni BMNPs catalyst supported on ZrO<sub>2</sub> for efficient and selective cleavage of  $\beta$ -O-4 ether linkage in lignin under ambient pressure and neutral conditions. ZrO<sub>2</sub> was chosen as the support because it appears to favor activation of O-compounds on support surface and to be essential for the hydrogen economy of the hydrogenolysis reaction, besides, amphoteric character of zirconia was reported to play a major role especially in preventing coke formation, which would be of great importance in HDO reaction.<sup>15</sup> To the best of our knowledge, this is the first example on the hydrogenolysis of  $\beta$ -O-4 ether linkages in lignin catalyzed by BMNPs using ordinary pressure hydrogen gas as the hydrogen source.

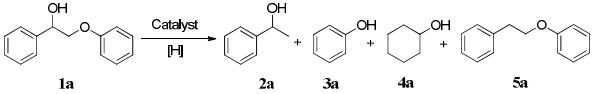
## Results and discussion

As a representative example, **1a** was selected as the model substrate to optimize the reaction conditions. Initially, PdNPs@ZrO<sub>2</sub> was used as the catalyst using 0.5 equiv NaBH<sub>4</sub> as the hydrogen source. The desired products (**2a** and **3a**) were generated in 37% yield with a trace of **5a** generated by the C-O bond cleavage of **1a** at  $\alpha$ -position, but the hydrogenation product **4a** of **3a** was not detected (Table 1, entry 1). Be mindful of the attractive properties of BMNPs, we attempted to apply PdNiNPs@ZrO<sub>2</sub> to upgrade the catalytic activity. As expected, dramatic enhancement in catalytic activity was observed (entries 1 vs 2), as benchmark, monometallic NiNPs@ZrO<sub>2</sub> only showed negligible activity in this reaction (entry 3), so we could conclude that Pd is the main active site in the BMNPs for the hydrogenolysis reaction. Simple mixture of PdNPs@ZrO<sub>2</sub> and NiNPs@ZrO<sub>2</sub> did not lead to marked increase in catalytic activity (entry 4), which highlights the importance of the synergistic effects for this reaction.

The results on the impact of the ratio of the two metals (entries 5-8) indicate that a higher percentage of nickel lead to a more active catalyst when the total loading of palladium is held constant in the reaction at 2.5 mol %, and Pd/Ni ratio of 1:8 was found to be the optimal presumably owing to the enhancement of hydrogen storage capacity.<sup>16</sup> Pd<sub>1</sub>Ni<sub>8</sub>NPs@ZrO<sub>2</sub> was detected by the inductively coupled plasma mass spectrometry (ICP-MS) (SI, Table S1), which confirmed that the Pd/Ni ratio was consistent with the designed composition of the Pd<sub>1</sub>Ni<sub>8</sub> BMNPs. Furthermore, the Pd loading of the catalyst was 0.71 wt.% indicating that the preparing method was effective without obvious dissipation of metal precursors. The

yield dropped dramatically (entry 9) when the Pd loading was reduced to 1.25 %. Following the similar preparation procedure, different BMNPs@ZrO<sub>2</sub> were prepared and employed as the catalysts in the hydrogenolysis (entries 10-15), Pd<sub>1</sub>Ni<sub>8</sub>NPs@ZrO<sub>2</sub> emerged as the best choice.

**Table 1** Optimization of the cleavage of  $\beta$ -O-4 linkage in **1a**.<sup>a</sup>



Entry	Catalyst	M <sub>1</sub> /M <sub>2</sub> (mol%)	<b>3a</b> % <sup>b</sup>	<b>4a</b> % <sup>b</sup>	<b>5a</b> % <sup>b</sup>
1	Pd	5/0	37	0	4
2	Pd <sub>1</sub> Ni <sub>2</sub>	5/10	95	0	5
3	Ni	0/10	trace	0	0
4	Pd/Ni	5/10	45	0	2
5	Pd <sub>1</sub> Ni <sub>4</sub>	2.5/10	57	0	7
6	Pd <sub>1</sub> Ni <sub>6</sub>	2.5/15	79	0	8
7	Pd <sub>1</sub> Ni <sub>8</sub>	2.5/20	96	0	4
8	Pd <sub>1</sub> Ni <sub>10</sub>	2.5/25	97	0	3
9	Pd <sub>1</sub> Ni <sub>8</sub>	1.25/10	14	0	4
10	Pd <sub>1</sub> Zn <sub>8</sub>	2.5/20	15	0	8
11	Pd <sub>1</sub> Cu <sub>8</sub>	2.5/20	34	0	5
12	Pd <sub>1</sub> Fe <sub>8</sub>	2.5/20	8	0	8
13	Pd <sub>1</sub> Co <sub>8</sub>	2.5/20	27	0	14
14	Ru <sub>1</sub> Ni <sub>8</sub>	2.5/20	35	0	12
15	Ir <sub>1</sub> Ni <sub>8</sub>	2.5/20	3	0	<2
16 <sup>c</sup>	Pd <sub>1</sub> Ni <sub>8</sub>	2.5/20	26	0	11
17 <sup>d</sup>	Pd <sub>1</sub> Ni <sub>8</sub>	2.5/20	65	0	9
18 <sup>e</sup>	Pd <sub>1</sub> Ni <sub>8</sub>	2.5/20	78	0	7
19 <sup>f</sup>	Pd <sub>1</sub> Ni <sub>8</sub>	2.5/20	38	0	13
20 <sup>g</sup>	Pd <sub>1</sub> Ni <sub>8</sub>	2.5/20	0	100	0
21 <sup>h</sup>	Pd <sub>1</sub> Ni <sub>8</sub>	2.5/20	56	42	2
22 <sup>h</sup>	Ni	0/22.5	26	8	9
23 <sup>h</sup>	Pd	22.5/0	17	75	8
24 <sup>i</sup>	Pd <sub>1</sub> Ni <sub>8</sub>	2.5/20	24	76	0
25 <sup>j</sup>	Pd <sub>1</sub> Ni <sub>8</sub>	2.5/20	0	100	0

<sup>a</sup> Reaction conditions: 0.5 mmol of **1a**, catalyst, 0.5 equiv NaBH<sub>4</sub>, 2 mL EtOH, 80 °C, 6 h. <sup>b</sup> Yields were determined by GC. <sup>c</sup> BmimCF<sub>3</sub>SO<sub>3</sub> was used as solvent. <sup>d</sup> 1,4-dioxane was used as solvent. <sup>e</sup> CH<sub>3</sub>CN was used as solvent. <sup>f</sup> H<sub>2</sub>O was used as solvent. <sup>g</sup> The hydrogen donor was hydrogen gas (supplied by a balloon of hydrogen gas), reaction time is 12 h instead of 6 h. <sup>h</sup> 2 equiv NaBH<sub>4</sub>. <sup>i</sup> 3 equiv NaBH<sub>4</sub>. <sup>j</sup> 5 equiv NaBH<sub>4</sub>.

After screening of different solvents, ethanol provided the best results due to its good polarity and Lewis basicity (entries 7, 16-19).<sup>17</sup> It should be noted that **1a** was totally cleaved and only **2a** and **4a** were found in the reaction when excessive amount of hydrogen gas was supplied by a balloon of

hydrogen gas (entry 20). Similar results were also observed in the presence of 5 equiv  $\text{NaBH}_4$  (entry 25). Based on results of further controlled experiments (entries 21–24), it can be concluded that (i)  $\text{PdNiNPs}@ZrO_2$  have excellent selectivity for the hydrolysis of  $\beta$ -O-4 linkage; (ii) the selectivity for the hydrogenation of phenol can be controlled by the amount of  $\text{NaBH}_4$ ,<sup>18</sup> (iii) the nickel in the BMNPs depresses the hydrogenation in a certain extent; (iv) no hydrogenation of **2a** or **5a** is found due to the mild conditions.

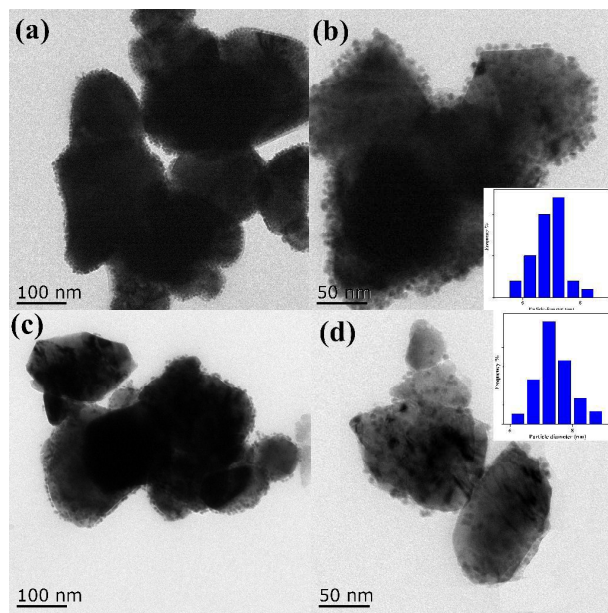


**Fig. 1** TEM images of (a) freshly prepared  $\text{Pd}_1\text{Ni}_8\text{NPs}@ZrO_2$  (b)  $\text{Pd}_1\text{Ni}_8\text{NPs}@ZrO_2$  after 10 cycles. The inset images show the size distribution of Pd-Ni bimetallic nanoparticles.

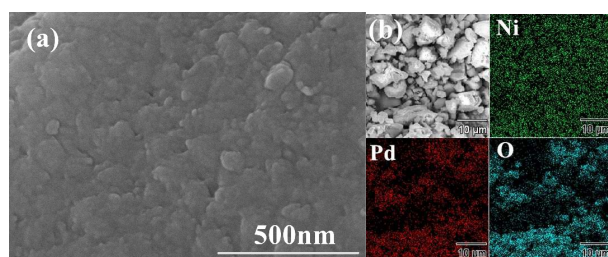


**Fig. 2** SEM image (a) and corresponding EDS elemental mappings (b) of  $\text{Pd}_1\text{Ni}_8\text{NPs}@ZrO_2$  catalyst in elements of Ni, Pd, O, respectively.

To investigate morphologies of the catalyst,  $\text{Pd}_1\text{Ni}_8\text{NPs}@ZrO_2$  was directly observed by transmission electron microscopy (TEM) and scanning electron microscopy (SEM). As shown in Fig. 1, the as prepared Pd-Ni BMNPs are well-proportioned anomalous spherical, and average size of the nanoparticles is about 6.9 nm and 7.3 nm for the fresh prepared and 10 cycle-samples, respectively. The TEM images also indicated that the BMNPs have a good dispersion on the surface of the matrix, which provides more contacting surface

area between active sites and substrates. The SEM images and area-selected SEM-EDS mappings of the catalyst are shown in Fig. 2, suggesting a uniform distribution and efficient loading of Ni and Pd elements on the surface of  $\text{ZrO}_2$ .

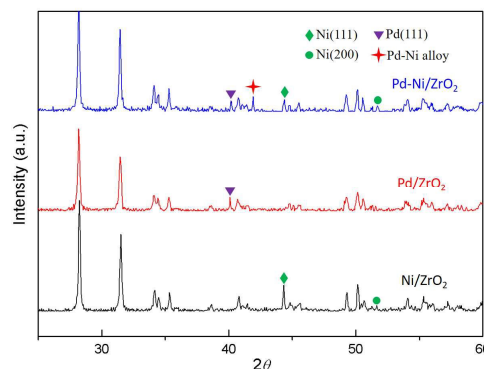


**Fig. 3** XRD patterns of  $\text{Ni}/ZrO_2$ ,  $\text{Pd}/ZrO_2$  and  $\text{Pd}_1\text{Ni}_8/ZrO_2$ .

The X-ray powder diffraction (XRD) patterns (Fig. 3) suggested that Pd-Ni particles contained a mixture of Ni (200), Ni (111) (JCPDS file: 65-0380) and Pd (111) (JCPDS file: 65-2867) phases, a small peak corresponding to the presence of a Pd-Ni alloy at a peak of  $\sim 41.9^\circ$  was also detected in the XRD pattern, indicating the formation of Pd-Ni alloy.<sup>19b</sup> Furthermore, the X-ray photoelectron spectrum (XPS) was also obtained to analyze the valence state of metal elements and the surface chemical composition of the  $\text{Pd}_1\text{Ni}_8\text{NPs}@ZrO_2$  catalyst (Fig. 4). The XPS spectra point out that the ratio of the surface concentration between Pd and Ni is 0.15, almost equal to the ICP-MS results. Together with the results of XRD and SEM-EDS, we could conclude that the Pd-Ni BMNPs are in a random homogeneous alloys form.<sup>13d,13e</sup> With several Ni atoms surrounded around Pd atoms, the hydrogen transfer ability of Pd is weakened, which makes great contributions to the inhibition in hydrogenation selectivity (geometric effects).<sup>19</sup>

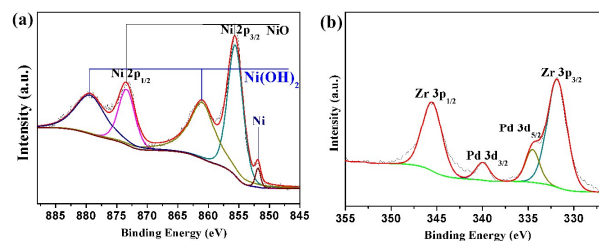


**Fig. 4** XPS spectrum of as-prepared  $\text{Pd}_1\text{Ni}_8\text{NPs}@ZrO_2$  catalyst: (a) Ni 2p region (b) Pd 3d region.

As shown in Fig. 4a, the Ni spectral feature of the catalyst consists of metallic Ni as well as Ni oxide and hydroxide.<sup>20</sup> The presence of NiO and  $\text{Ni(OH)}_2$  on the catalyst surface is ascribed to the fact that nickel can be easily oxidized and hydroxide when exposed to oxygen and moisture in air. As reported by Zhang et al., inert metal oxide on the BMNPs surface can

## COMMUNICATION

segregate its terrace zones, thus preventing benzene ring coordination and hydrogenation, which may have a significant contribution for the selectivity of the BMNPs due to the "blockage effect".<sup>21</sup> As illustrated in Fig. 3b, peaks located at 335.4 ± 0.2 eV and 341.0 ± 0.2 eV can be assigned to Pd3d<sub>5/2</sub> and Pd3d<sub>3/2</sub>, which further confirmed the formation of Pd-Ni alloy in the Pd<sub>1</sub>Ni<sub>8</sub>NPs@ZrO<sub>2</sub> catalyst.<sup>22</sup> A peak shift (about 0.2 eV) of Pd 3d<sub>5/2</sub> in binding energy in Pd<sub>1</sub>Ni<sub>8</sub>@ZrO<sub>2</sub> catalyst was observed, indicating an electronic structure modification of Pd active sites by addition of Ni.<sup>23</sup> The mixed peak of Pd 3p<sub>3/2</sub> and O 1s was deconvoluted into Pd 3p<sub>3/2</sub> at 529.5 eV and O 1s at 531.2 eV (SI, Fig. S1), the main O 1s feature at 531.2 eV arises from the high concentration of oxygen in the support.<sup>24</sup> The formation of bimetallic nanoparticles could accelerate the electron transformation from Pd to Ni, which creates more electron-rich Ni sites. The electron-rich Ni center may spur the conversion from H• to H-, which significantly speeds up the hydrogenolysis process (electronic effects).<sup>14a,18</sup> According to those results, we could propose that Ni and Pd have promotion for each other in the hydrogenolysis reaction through formation of alloy NPs.

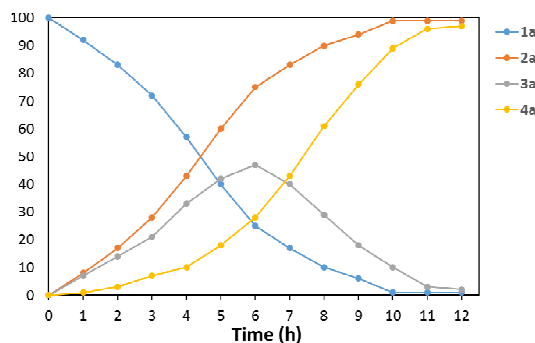
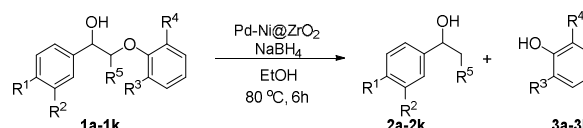


Fig. 5 Product distributions as functions of time for hydrogenolysis of **1a** under optimized conditions.

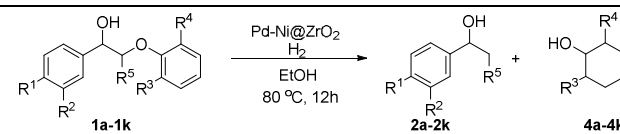
To gain preliminary insights into the reaction mechanism, a model reaction with **1a** as the substrate was conducted under optimized conditions (Table 1, entry 20) and tracked by GC and GC-MS (Fig. 5). As showcased in the Fig. 5, **1a** was gradually converted into the products **2a** and **3a** with time. The hydrogenation product **4a** generated when the reaction started was at a negligible level but it gradually increased as the reaction proceeded, and **4a** attained the highest yield at the end of the reaction, which indicates that hydrogenation of the benzene ring occurs after hydrogenolysis of the  $\beta$ -O-4 ether linkages.

With the optimized reaction conditions in hands, we next investigated the  $\beta$ -O-4 bond cleavage in more detail by varying the ether substituents. Gratifyingly, introducing one methoxy group at R<sup>3</sup> or R<sup>4</sup> positions have no passive influence on the yield (Table 2, entry 2). A slightly decrease of yields was observed when R<sup>1</sup> or R<sup>2</sup> was substituted with methoxy group (entries 3,4), which can be explained by the increased BDE of  $\beta$ -O-4 linkage.<sup>25</sup> For the substrates bearing two or more methoxy group, promising yields were afforded (entries 5-9). Less bulk substrate with a methyl at R<sup>1</sup>

Table 2 Ni-Pd BMNPs catalyzed  $\beta$ -O-4 cleavage of various lignin models.



Entry	1	R <sup>1</sup>	R <sup>2</sup>	R <sup>3</sup>	R <sup>4</sup>	R <sup>5</sup>	Yield [%] <sup>f</sup>
1 <sup>a</sup>	<b>1a</b>	H	H	H	H	H	100
2 <sup>a</sup>	<b>1b</b>	H	H	H	OMe	H	97
3 <sup>a</sup>	<b>1c</b>	OMe	H	H	H	H	86
4 <sup>a</sup>	<b>1d</b>	H	OMe	H	H	H	83
5 <sup>a</sup>	<b>1e</b>	H	OMe	H	OMe	H	81
6 <sup>a</sup>	<b>1f</b>	OMe	H	H	OMe	H	94
7 <sup>a</sup>	<b>1g</b>	H	H	OMe	OMe	H	92
8 <sup>a</sup>	<b>1h</b>	OMe	H	OMe	OMe	H	81
9 <sup>a</sup>	<b>1i</b>	H	OMe	OMe	OMe	H	84
10 <sup>a</sup>	<b>1j</b>	Me	H	H	H	H	92
11 <sup>a</sup>	<b>1k</b>	F	H	H	H	H	>99
12 <sup>a</sup>	<b>1l</b>	OMe	OMe	OMe	H	CH <sub>2</sub> OH	80



Entry	1	R <sup>1</sup>	R <sup>2</sup>	R <sup>3</sup>	R <sup>4</sup>	R <sup>5</sup>	Yield [%] <sup>f</sup>
13 <sup>b</sup>	<b>1a</b>	H	H	H	H	H	98
14 <sup>b</sup>	<b>1b</b>	H	H	H	OMe	H	96
15 <sup>b</sup>	<b>1c</b>	OMe	H	H	H	H	85
16 <sup>b</sup>	<b>1d</b>	H	OMe	H	H	H	83
17 <sup>b</sup>	<b>1e</b>	H	OMe	H	OMe	H	78
18 <sup>b</sup>	<b>1f</b>	OMe	H	H	OMe	H	87
19 <sup>b</sup>	<b>1g</b>	H	H	OMe	OMe	H	89
20 <sup>b</sup>	<b>1h</b>	OMe	H	OMe	OMe	H	81
21 <sup>b</sup>	<b>1i</b>	H	OMe	OMe	OMe	H	84
22 <sup>b</sup>	<b>1j</b>	Me	H	H	H	H	92
23 <sup>b</sup>	<b>1k</b>	F	H	H	H	H	97
24 <sup>b</sup>	<b>1l</b>	OMe	OMe	OMe	H	CH <sub>2</sub> OH	73

<sup>a</sup> Reaction conditions: 0.5 mmol of substrate, 2.5% catalyst (catalyst amount was based on palladium), 0.25 mmol NaBH<sub>4</sub>, 80 °C, 6 h. <sup>b</sup> The hydrogen donor was H<sub>2</sub> (supplied by a hydrogen balloon). <sup>c</sup> Yields were determined by GC.

position also underwent efficient fragmentation (entry 10). Moreover, substrate with an electron-withdrawing group at R<sup>1</sup> position can also be efficiently fragmented (entry 11). Besides, to exactly mimic the lignin,  $\beta$ -O-4 model compound with  $\gamma$ -CH<sub>2</sub>OH (**1l**) was also tested for the reaction, satisfactory yield was obtained (entry 12). Similar reaction regularities were observed using H<sub>2</sub> as the hydrogen source, but the produced

phenols were hydrogenated into cyclohexanol sequentially due to excessive amount of H<sub>2</sub> (entries 13-24).

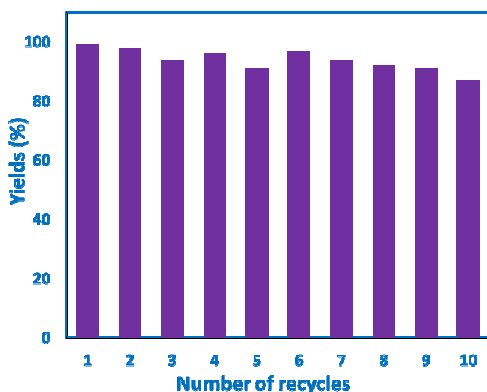


Fig. 6 Recycling of Pd<sub>1</sub>Ni<sub>8</sub>NPs@ZrO<sub>2</sub> in the hydrogenolysis of 2-phenoxy-1-phenylethanol.

The reusability of the Pd<sub>1</sub>Ni<sub>8</sub>NPs@ZrO<sub>2</sub> catalyst system was also investigated using **1a** as the substrate (5 mmol scale) under the optimized conditions (Table 1, entry 20). After the reaction completes, the catalyst can be easily separated by simple filtration and directly reused in the next cycle after washed with water and ethanol. After the catalyst was recycled for 5 times, 5% of the catalyst was added to make up the catalyst loss during the recycled process. This process could be repeated at least ten times without decrease in activity (Fig. 6). The heterogeneous nature of PdNiNPs@ZrO<sub>2</sub> catalyst was demonstrated by a hot filtration experiment (Fig. 7). The catalyst was filtered off after 2 h at 80 °C, and the isolated solution was allowed to react for further 2 h under identical conditions. No further increase in yield was observed. Addition of the removed catalyst led to resumption of the reaction. These experiments indicate that PdNiNPs@ZrO<sub>2</sub> exhibits excellent stability and recyclability and metal leaching of the catalyst is negligible during hydrogenolysis process.

Encouraged by the remarkable results on the lignin model compounds and the good stability of the catalyst, we next performed the catalyst in the hydrogenolysis of organosolv lignin extracted from birch sawdust.<sup>26</sup> The reaction conditions were similar to the hydrogenolysis of model compounds using H<sub>2</sub> as the hydrogen source except that the reaction time was prolonged to 24 h. The catalyst and the insoluble residue was filtered and washed with ethyl acetate, and the filtrate was washed with water. A soluble fraction (control experiments were performed to exclude the soluble fraction of initial organosolv lignin), corresponding to 56 wt.% of the original lignin, was obtained (Fig. 8). The soluble fraction, containing the majority of the lignin derived mass was analyzed by GC-MS (SI, Fig. S2) and 2D HSQC NMR (SI, Fig. S4). As shown in the GC-MS spectra, three major products were obtained and plausible structures of the three major components were present in Fig. S3 (SI).<sup>5d,14a,27</sup> Together with the 2D HSQC NMR, in which the characteristic signals of β-O-4 linkages almost disappeared entirely, we could conclude that lignin has been

selectively depolymerized under our mild reaction condition. Attempts were also made to recycle the catalyst in the hydrogenolysis of lignin. Not unexpectedly, the catalyst can be reused for at least 5 times under identical conditions (Fig. 8), which is appealing and significant for the large-scale operations, distribution of major products after each cycle can be found Table S2 (SI).

In summary, highly dispersed Pd-Ni BMNPs immobilized on ZrO<sub>2</sub> prove to be an effective catalyst for the hydrogenolysis of β-O-4 linkage in lignin under H<sub>2</sub> at atmospheric pressure with excellent selectivity. Alloying palladium with nickel leads to superior activity enhancement over corresponding mono-metallic catalyst and lower selectivity of hydrogenation than palladium based on experimental and characterization results highlighting remarkable “synergistic effects”. The hydrogenation of the produced phenols is mainly controlled by tuning the amount of hydrogen donor (NaBH<sub>4</sub>) introduced, which is valuable to selectively obtain desired products in the basis of different applications. Furthermore, these procedures are performed under mild conditions using a recyclable catalyst, thereby offering considerable potentials for large-scale operations of the lignin depolymerization. Ongoing efforts are dedicated to understand the origin of the enhanced activity and selectivity so as to guide future design of the optimal catalysts.

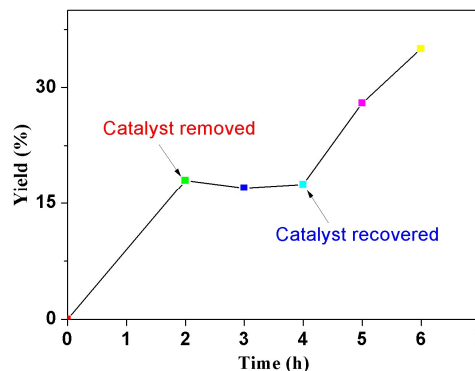


Fig. 7 Hot filtration experiments of Pd<sub>1</sub>Ni<sub>8</sub>NPs@ZrO<sub>2</sub> for hydrogenolysis of 2-phenoxy-1-phenylethanol.

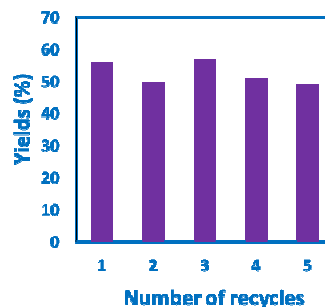


Fig. 8 Recycling of Pd<sub>1</sub>Ni<sub>8</sub>NPs@ZrO<sub>2</sub> in depolymerization of birch lignin.

## Acknowledgements

We gratefully acknowledge Nature Science Foundation of Jiangsu Province (BK 20140776) the Fundamental Research Funds for the Central Universities (30915011315) for financial support. This work was also supported by National Natural Science Foundation of China (21476116, 21402093) and Chinese Postdoctoral Science Foundation (2015M571761, 2016T90465) for financial support.

## Notes and references

- (a) A. J. Ragauskas, C. K. Williams, B. H. Davison, G. Britovsek, J. Cairney, C. A. Eckert, W. J. Frederick, J. P. Hallett, D. J. Leak, C. L. Liotta, J. R. Mielenz, R. Murphy, R. Templer and T. Tschaplinski, *Science*, 2006, **311**, 484-489; (b) D. Q. Ding, J. X. Xi, J. J. Wang, X. H. Liu, G. Z. Lu and Y. Q. Wang, *Green Chem.*, 2015, **17**, 4037-4044; (c) Y.-H. P. Zhang, *J. Ind. Microbiol. Biotechnol.*, 2008, **35**, 367-375; (d) M. FitzPatrick, P. Champagne, M. F. Cunningham and R. A. Whitney, *Bioresour. Technol.*, 2010, **101**, 8915-8922; (e) A. Ghosh, R. C. Brown and X. Bai, *Green Chem.*, 2016, **18**, 1023-1031; (f) Y. Wang, S. De and N. Yan, *Chem. Commun.*, 2016, **52**, 6210-6224.
- (a) S. H. Li, S. Q. Liu, J. C. Colmenares and Y. J. Xu, *Green Chem.*, 2016, **18**, 594-607; (b) J. Larsen, M. Ø. Haven and L. Thirup, *Biomass Bioenergy*, 2012, **46**, 36-45; (c) C. Xu, R. A. D. Arancon, J. Labidi and R. Luque, *Chem. Soc. Rev.*, 2014, **43**, 7485-7500; (d) S. Dabral, J. Mottweiler, T. Rinesch and C. Bolm, *Green Chem.*, 2015, **17**, 4908-4912.
- (a) B. Sedai, C. Díaz-Urrutia, R. T. Baker, R. Wu, L. A. P. Silks and S. K. Hanson, *ACS Catal.*, 2011, **1**, 794-804; (b) S. K. Hanson, R. Wu and L. A. P. Silks, *Angew. Chem. Int. Ed.*, 2012, **51**, 3410-3413; (c) B. Sedai, C. Díaz-Urrutia, R. T. Baker, R. Wu, L. A. P. Silks and S. K. Hanson, *ACS Catal.*, 2013, **3**, 3111-3122; (d) J. M. Nichols, L. M. Bishop, R. G. Bergman and J. A. Ellman, *J. Am. Chem. Soc.*, 2010, **132**, 12554-12555; (e) J. M. W. Chan, S. Bauer, H. Sorek, S. Sreekumar, K. Wang and F. D. Toste, *ACS Catal.*, 2013, **3**, 1369-1377; (f) T. B. Mike Kleinert, *Energy Fuels*, 2008, 1371-1379.
- (a) C. O. Tuck, E. Pérez, I. T. Horváth, R. A. Sheldon and M. Poliakoff, *Science*, 2012, **337**, 695-699; (b) R. Beauchet, F. Monteil-Rivera and J. M. Lavoie, *Bioresour. Technol.*, 2012, **121**, 328-334.
- (a) L. Chen, J. Y. Xin, L. L. Ni, H. X. Dong, D. X. Yan, X. M. Lu and S. J. Zhang, *Green Chem.*, 2016, **18**, 2341-2352; (b) A. J. Ragauskas, G. T. Beckham, M. J. Biddy, R. Chandra, F. Chen, M. F. Davis, B. H. Davison, R. A. Dixon, P. Gilna, M. Keller, P. Langan, A. K. Naskar, J. N. Saddler, T. J. Tschaplinski, G. A. Tuskan and C. E. Wyman, *Science*, 2014, **344**, 709-719; (c) D. R. Dodds and R. A. Gross, *Science*, 2007, **318**, 1250-1251; (d) C. Li, X. Zhao, A. Wang, G. W. Huber and T. Zhang, *Chem. Rev.* 2015, **115**, 11559-11624.
- Y. S. Choi, R. Singh, J. Zhang, G. Balasubramanian, M. R. Sturgeon, R. Katahira, G. Chupka, G. T. Beckham and B. H. Shanks, *Green Chem.*, 2016, **18**, 1762-1773.
- (a) T. L. Lohr, Z. Li and T. J. Marks, *ACS Catal.*, 2015, **5**, 7004-7007; (b) Z. C. Luo and C. Zhao, *Catal. Sci. Technol.*, 2016, **6**, 3476-3484; (c) J. Zhang, Y. Liu, S. Chiba and T. P. Loh, *Chem. Commun.*, 2013, **49**, 11439-11441; (d) J. He, C. Zhao and J. A. Lercher, *J. Am. Chem. Soc.*, 2012, **134**, 20768-20775.
- (a) A. M. Ruppert, K. Weinberg and R. Palkovits, *Angew. Chem. Int. Ed. Engl.*, 2012, **51**, 2564-2601; (b) M. Zaheer and R. Kempe, *ACS Catal.*, 2015, **5**, 1675-1684; (c) Q. Song, F. Wang, J. Cai, Y. Wang, J. Zhang, W. Yu and J. Xu, *Energ. Environ. Sci.*, 2013, **6**, 994-1007; (d) X. Huang, T. I. Koranyi, M. D. Boot and E. J. M. Hensen, *Green Chem.*, 2015, **17**, 4941-4950; (e) J. S. Kruger, N. S. Cleveland, S. T. Zhang, R. Katahira, B. A. Black, G. M. Chupka, T. Lammens, P. G. Hamilton, M. J. Biddy and G. T. Beckham, *ACS Catal.*, 2016, **6**, 1316-1328.
- (a) M. V. Galkin, C. Dahlstrand and J. S. Samec, *ChemSusChem*, 2015, **8**, 2187-2192; (b) P. Dong, G.-p. Lu and C. Cai, *New J. Chem.*, 2016, **40**, 1605-1609.
- (a) A. G. Sergeev and J. F. Hartwig, *Science*, 2011, **332**, 439-443; (b) A. G. Sergeev, J. D. Webb and J. F. Hartwig, *J. Am. Chem. Soc.*, 2012, **134**, 20226-20229; (c) J. G. Zhang, H. Asakura, J. van Rijn, J. Yang, P. Duchesne, B. Zhang, X. Chen, P. Zhang, M. Saeys and N. Yan, *Green Chem.*, 2014, **16**, 2432-2437; (d) E. Feghali and T. Cantat, *Chem. Commun.*, 2014, **50**, 862-865; (e) V. Molinari, G. Clavel, M. Graglia, M. Antonietti and D. Esposito, *ACS Catal.*, 2016, **6**, 1663-1670.
- (a) B. M. Rosen, K. W. Quasdorf, D. A. Wilson, N. Zhang, A.-M. Resmerita, N. K. Garg and V. Percec, *Chem. Rev.*, 2011, **111**, 1346-1416; (b) Y.-B. Huang, L. Yan, M.-Y. Chen, Q.-X. Guo and Y. Fu, *Green Chem.*, 2015, **17**, 3010-3017; (c) V. M. Roberts, R. T. Knapp, X. Li and J. A. Lercher, *ChemCatChem*, 2010, **2**, 1407-1410; (d) V. M. Roberts, V. Stein, T. Reiner, A. Lemonidou, X. Li and J. A. Lercher, *Chem. Eur. J.*, 2011, **17**, 5939-5948; (e) V. Roberts, S. Fendt, A. A. Lemonidou, X. Li and J. A. Lercher, *Appl. Catal. B*, 2010, **95**, 71-77; (f) L. Shuai and J. Luterbacher, *ChemSusChem*, 2016, **9**, 133-155.
- (a) J. A. Rodriguez and D. W. Goodman, *Science*, 1992, **257**, 897-903; (b) M. Jaime, R. Movshovich, G. R. Stewart, W. P. Beyersmann, M. G. Berisso, M. F. Hundley, P. C. Canfield and J. L. Sarrao, *Nature*, 2000, **405**, 160-163.
- (a) Y. Wu, S. Cai, D. Wang, W. He and Y. Li, *J. Am. Chem. Soc.*, 2012, **134**, 8975-8981; (b) I. Nakamura, Y. Yamanoi, T. Imaoka, K. Yamamoto and H. Nishihara, *Angew. Chem. Int. Ed.*, 2011, **50**, 5830-5833; (c) S. Cai, H. Duan, H. Rong, D. Wang, L. Li, W. He and Y. Li, *ACS Catal.*, 2013, **3**, 608-612; (d) D. Wang and Y. Li, *Adv. Mater.*, 2011, **23**, 1044-1060; (e) M. Sankar, N. Dimitratos, P. J. Miedziank, P. P. Wells, C. J. Kiely and G. J. Hutchings, *Chem. Soc. Rev.*, 2012, **41**, 8099-8139.
- (a) J. Zhang, J. Teo, X. Chen, H. Asakura, T. Tanaka, K. Teramura and N. Yan, *ACS Catal.*, 2014, **4**, 1574-1583; (b) H. Konnerth, J. Zhang, D. Ma, M. H. G. Precht and N. Yan, *Chem. Eng. Sci.*, 2015, **123**, 155-163; (c) J. Zhang and N. Yan, *Part. Part. Syst. Char.*, 2016, **33**, 610-619.
- (a) V. A. Yakovlev, S. A. Khromova, O. V. Sherstyuk, V. O. Dundich, D. Y. Ermakov, V. M. Novopashina, M. Y. Lebedev, O. Bulavchenko and V. N. Parmon, *Catal. Today*, 2009, **144**, 362-366; (b) V. N. Bui, D. Laurenti, P. Delichère and C. Geantet, *Applied Catal. B Environ.*, 2011, **101**, 246-255.
- V. Udumula, J. H. Tyler, D. A. Davis, H. Wang, M. R. Linford, P. S. Minson and D. J. Michaelis, *ACS Catal.*, 2015, **5**, 3457-3462.
- X. Wang and R. Rinaldi, *ChemSusChem*, 2012, **5**, 1455-1466.
- In fact, we have also tried to eliminate the hydrogenation of phenol by reducing the amount of H<sub>2</sub>, but no satisfactory result was obtained because we cannot detect the amount of H<sub>2</sub> in balloon. We believe that a 100% selectivity for the products **3a** can be achieved by regulating the amount of H<sub>2</sub> with specific equipment.
- (a) D. M. Alonso, S. G. Wettstein and J. A. Dumesic, *Chem. Soc. Rev.*, 2012, **41**, 8075-8098; (b) J. J. Zhang and C. Zhao, *ACS Catalysis*, 2016, **6**, 4512-4525.
- (a) J. Xia, G. He, L. Zhang, X. Sun and X. Wang, *Applied Catal. B Environ.*, 2016, **180**, 408-415; (b) J.-w. Zhang, G.-p. Lu and C. Cai, *Catal. Commun.*, 2016, **84**, 25-29.
- J. Zhang, M. Ibrahim, V. Collière, H. Asakura, T. Tanaka, K. Teramura, K. Philippot and N. Yan, *J. Mol. Catal. A: Chem.*, 2016, **422**, 188-197.
- (a) G. Beketov, B. Heinrichs, J. P. Pirard, S. Chenakin and N. Kruse, *Appl. Surf. Sci.*, 2013, **287**, 293-298; (b) M. A. Arellano-

## Journal Name COMMUNICATION

- González, A. C. Texier, L. Lartundo-Rojas and I. González, *J. Electrochem. Soc.*, 2015, **162**, E223-E230.
- 23 L. T. M. Nguyen, H. Park, M. Banu, J. Y. Kim, D. H. Youn, G. Magesh, W. Y. Kim and J. S. Lee, *RSC Adv.*, 2015, **5**, 105560-105566.
- 24 Y. Matsumura, M. Okumura, Y. Usami, K. Kagawa, H. Yamashita, M. Anpo and M. Haruta, *Catal. Lett.*, 1997, **44**, 189-191.
- 25 S. Kim, S. C. Chmely, M. R. Nimlos, Y. J. Bomble, T. D. Foust, R. S. Paton and G. T. Beckham, *J. Phys. Chem. Lett.*, 2011, **2**, 2846-2852.
- 26 The organosolv lignin was obtained according a pervious report as follow: C. S. Lancefield, O. S. Ojo, F. Tran and N. J. Westwood, *Angew. Chem. Int. Ed.*, 2015, **54**, 258-262.
- 27 A. Rahimi, A. Ulbrich, J. J. Coon and S. S. Stahl, *Nature*, 2014, **515**, 249-252.

